Chinese Chemical Letters 31 (2020) 996–999

Contents lists available at ScienceDirect

Chinese Chemical Letters

journal homepage: www.elsevier.com/locate/cclet

Communication

Mechanical properties and frictional resistance of Al composites reinforced with $Ti_3C_2T_x$ MXene

Jie Hu, Shibo Li*, Jing Zhang, Qiuying Chang, Wenbo Yu, Yang Zhou

School of Mechanical and Electronic Control Engineering, Beijing Jiaotong University, Beijing 100044, China

ARTICLE INFO

Article history:
Received 10 August 2019
Received in revised form 29 August 2019
Accepted 30 August 2019
Available online 4 September 2019

Keywords:
$Ti_3C_2T_x$ Mxene
Al composites
Microstructure
Mechanical properties
Frictional properties

ABSTRACT

Two-dimensional (2D) $Ti_3C_2T_x$ MXene is an attractive additive not only used in base oil due to its low friction coefficient, but also used in composites due to its high aspect ratio and rich surface functional groups. So far there has been intense research into polymer matrix composites reinforced with $Ti_3C_2T_x$. Here we report on the use of 2D $Ti_3C_2T_x$ to enhance the mechanical and frictional properties of Al matrix composites. $Ti_3C_2T_x$/Al composites were designed and prepared by pressureless sintering followed by hot extrusion technique. The prepared composites exhibit a homogeneous distribution of $Ti_3C_2T_x$. The Vickers hardness and the tensile strength continuously increase with increasing $Ti_3C_2T_x$ content. A hardness of 0.52 GPa and a tensile strength of 148 MPa were achieved in the 3 wt% $Ti_3C_2T_x$/Al composite. The frictional properties of pure Al and the $Ti_3C_2T_x$/Al composite were comparably studied under dry sliding. A low friction coefficient of 0.2, twice lower than that of pure Al, was achieved in the 3 wt% $Ti_3C_2T_x$/Al composite. $Ti_3C_2T_x$ acting as a solid lubricant reduces the abrasive wear in the composite, improving the frictional properties of Al matrix composites.

Aluminium matrix composites have been widely used in automotive, marine, building, packaging, electronic and aerospace industries due to their light weight, good mechanical properties, good machinability, good thermal and electrical conductivities, and other attractive properties. Al matrix composites with improved properties through the incorporation of graphene and carbon nanotubes (CNTs) have prompted intense research [1,2]. However, there are still scientific and technical challenges that must be overcome. First, graphene and CNTs are easily agglomerated. Homogeneous distribution in Al matrix without damaging the structures of graphene and CNTs is required. Second, the poor affinity of carbon materials with Al induces weak interfacial bonding in the composites. Third, interfacial reactions between carbon materials and Al matrix induce the formation of brittle and hygroscopic Al_4C_3, causing the structural damage of nanoscale reinforcements [3–5]. To homogeneously disperse the graphene and CNTs in Al matrix, many processing methods have been developed, *e.g.*, liquid metallurgy, thermal spray, mechanical alloying, electrochemical deposition, molecular level mixing, and stir friction processing [1,2,6–10]. To improve the wettability of graphene and CNTs with metal matrix, metallic coatings (Cu or Ni) on graphene and CNTs [6,11] and surface modification of CNTs by -O and -OH functional groups [12,13] have been adopted. The surface-modified CNTs and graphene have good wettability with metal matrices, further promoting their uniform distribution in the metal matrix composites.

Recently, a new class of two-dimensional (2D) MXenes, similar to graphene, has attracted much attention due to their unique combination of mechanical, electrical, optical, and electrochemical properties. The MXene materials have exciting potential applications in energy storage, electromagnetic interference shielding, water purification, sensors, lubrication, and reinforcement for composites [14–21].

In the MXene family, $Ti_3C_2T_x$ (T_x represents the terminal groups such as hydroxyl (-OH), oxide (-O) or fluorine (-F), x is the number of terminal groups) is the first discovered one obtained by HF-etching the Al layers from Ti_3AlC_2 [21]. The surface functional groups and high specific surface area to volume ratio make $Ti_3C_2T_x$ attractive as an additive in composites. The rich functional groups of $Ti_3C_2T_x$ enhance the matrix-filler interface bonding, improving the mechanical properties and electrical conductivities of polymer composites [22–27]. Up to date, most work has focused on polymer composites reinforced with $Ti_3C_2T_x$. There are a few of reports on the incorporation of $Ti_3C_2T_x$ in ceramic and metal matrix composites with improved mechanical properties. For example, the fracture toughness, flexural strength, and hardness of 2 wt%

* Corresponding author.
E-mail address: shbli1@bjtu.edu.cn (S. Li).

https://doi.org/10.1016/j.cclet.2019.09.004

$Ti_3C_2T_x/Al_2O_3$ composite has been improved by 300%, 150% and 300%, respectively [28]. The tensile strength of 5 vol% $Ti_3C_2T_x$/Cu composite has been improved by 40%, and its wear resistance has been greatly improved [29]. The above studies demonstrate that the $Ti_3C_2T_x$ MXene is an attractive material for reinforcement of polymer, metal and ceramic matrix composites.

Our previous work showed that $Ti_3C_2T_x$ is thermally stable with Al at temperatures below 700 °C, and strong interface bonding between $Ti_3C_2T_x$ and Al is achieved [30]. Therefore, properties of Al composites reinforced with $Ti_3C_2T_x$ are expected to be enhanced. In comparison to graphene and CNTs, $Ti_3C_2T_x$ offers obvious advantages to reinforce Al composites. The easy fabrication of $Ti_3C_2T_x$ from Ti_3AlC_2 makes the low-cost of production. In addition, the surface functional groups of -O, -OH and -F enhance the wettability of $Ti_3C_2T_x$ with Al matrix. This guarantees the uniform distribution of $Ti_3C_2T_x$ in Al matrix and the strong interfacial bonding in composites. In the present study, pressureless sintering followed by hot-extrusion was adopted to prepare $Ti_3C_2T_x$/Al composites. The mechanical and frictional properties of composites were investigated. Scanning electron microscopy was used to characterize the microstructure.

To fabricate $Ti_3C_2T_x$ MXene, Ti_3AlC_2 as precursor powder was selectively etched by 40% HF solution at 50 °C for 0.5 h. The processing has been described in detail elsewhere [30].

$Ti_3C_2T_x$ with contents ranging from 0.5 wt% to 3 wt% was mixed with Al in polypropylene containers for 10 h in a ball-miller. The mixtures were cold-pressed into green compacts with dimensions of 20 mm in diameter and 15–20 mm in height, under a pressure of 100 MPa. The green compacts were pressurelessly sintered in a graphite crucible coated with boron nitride at 650 °C for 1 h in Ar. Subsequently, the sintered samples (Fig. S1a in Supporting information) were subjected to hot extrusion at 460 °C. During extrusion processing, graphite-based oil as lubricant was applied between samples and dies. The extrusion speed was 5 mm/min, and the extrusion ratio was about 10:1 (the ratio of cross sectional areas before and after hot extrusion). The extruded bar with a cross-sectional area of 3×10 mm^2 was illustrated in Fig. S1b (Supporting information). For comparison, pure Al material was also prepared under the same processing conditions. The extruded bars were machined into specimens. The surfaces of specimens were polished to 0.5 μm with diamond paste for tensile and friction testing.

Tensile testing was conducted in a WDW-100E test machine. The shape and size of specimens for tensile test was presented in Fig. S1c (Supporting information). The tensile speed was 0.2 mm/min. At least 3 bars were tested to determine an average value of tensile strength.

The hardness measurement was done using a TH700 hardness tester. The hardness indentations were operated at a load of 5 kg and a dwell time of 15 s. Six measurements in different areas were taken under the same load to obtain an average value of hardness.

Friction testing was performed in a MFT-5000 machine with a ball-on-plate configuration. The ball is made of GCr15 bearing steel with a hardness of 62–67 HRC. The ball was pressed with a load of 5 N against Al and $Ti_3C_2T_x$/Al samples. The rotational speed was 800 rpm. The test was run for 5 min and the running distance was about 125 m.

The microstructures of samples as well as their fracture and worn surfaces were observed with scanning electron microscopy (SEM, ZEISS EVO 18, Carl Zeiss SMT, Germany) equipped with an energy-dispersive spectrometer system (EDS).

The backscattered SEM micrograph shows the microstructure of 3 wt% $Ti_3C_2T_x$/Al composite (Fig. 1a). There are no agglomerated $Ti_3C_2T_x$ particles (light gray), indicating a homogeneous distribution of $Ti_3C_2T_x$ in Al matrix composite. The EDS analysis presents the elemental distribution in the selected area containing a $Ti_3C_2T_x$ particle (Fig. 1b). The $Ti_3C_2T_x$ particle is mainly composed of Ti, C, F and O, suggesting that $Ti_3C_2T_x$ distributing in Al matrix is mainly terminated with -F and -O functional groups. The pristine $Ti_3C_2T_x$ particles have -F, -O and -OH surface groups after etching in HF solution. However, the -OH group is easily removed after heat treating at 650 °C [30].

Fig. 2 shows the mechanical properties as a function of $Ti_3C_2T_x$ content. Both the Vickers hardness and the tensile strength continuously increased with increasing $Ti_3C_2T_x$ content (Figs. 2a and b). As the content of $Ti_3C_2T_x$ is raised to 3 wt%, the $Ti_3C_2T_x$/Al composite has a hardness of 0.52 GPa and a tensile strength of 148 MPa, increased by 92% and 50%, respectively. The above result indicates that $Ti_3C_2T_x$ is an effective reinforcement in Al matrix composite, which should be ascribed to the homogeneous distribution of $Ti_3C_2T_x$ and the strong interface bonding between $Ti_3C_2T_x$ and Al matrix. The increase tendency indicates that the mechanical properties of the $Ti_3C_2T_x$/Al composites may be further improved if the content of $Ti_3C_2T_x$ exceeds 3 wt%. This work will be performed.

Fig. 3 presents the fracture surfaces of 3 wt% $Ti_3C_2T_x$/Al composite after tensile test. Fine dimples are present in the fracture surfaces (Figs. 3a and b), suggesting that the fracture mode is partially ductile. Some large pores are found (Fig. 3b), which might be resulted from the pull-out of $Ti_3C_2T_x$. This presumption was confirmed by the microstructure shown in Fig. 3c where the pulled-out $Ti_3C_2T_x$ particles on the fracture surface are obvious. This feature also reveals that a part of $Ti_3C_2T_x$ particles bonds strongly with Al matrix. Some $Ti_3C_2T_x$ particles are fractured and delaminated, with kinked layers (marked with an arrow in Fig. 3d).

During the tensile test, Al matrix plastically deforms, and small microvoids form under the applied stress. As deformation continues, these microvoids enlarge and coalesce to form an elliptical crack. The propagation of crack induces the fracture of Al matrix with the appearance of dimples. During Al deformation, the applied stress will be gradually transferred to the $Ti_3C_2T_x$

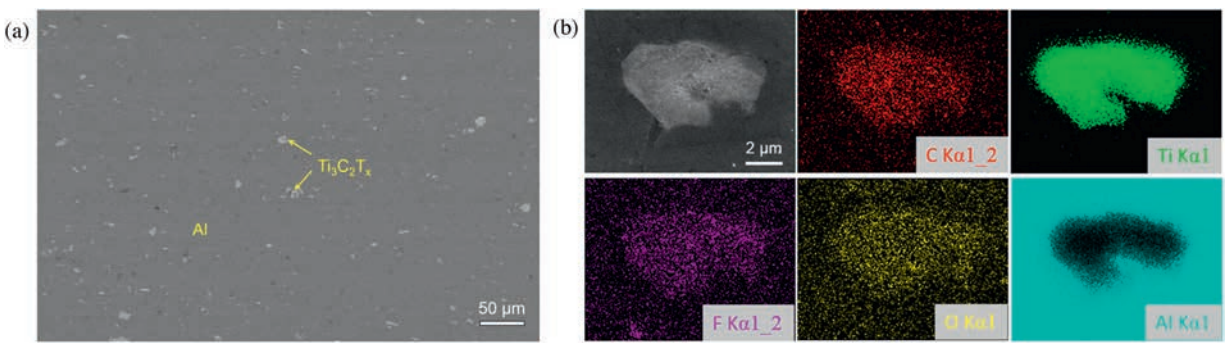

Fig. 1. (a) Backscattered SEM micrograph of the polished surface of 3 wt% $Ti_3C_2T_x$/Al composite. (b) EDS maps for the distribution of C, Ti, F, O and Al.

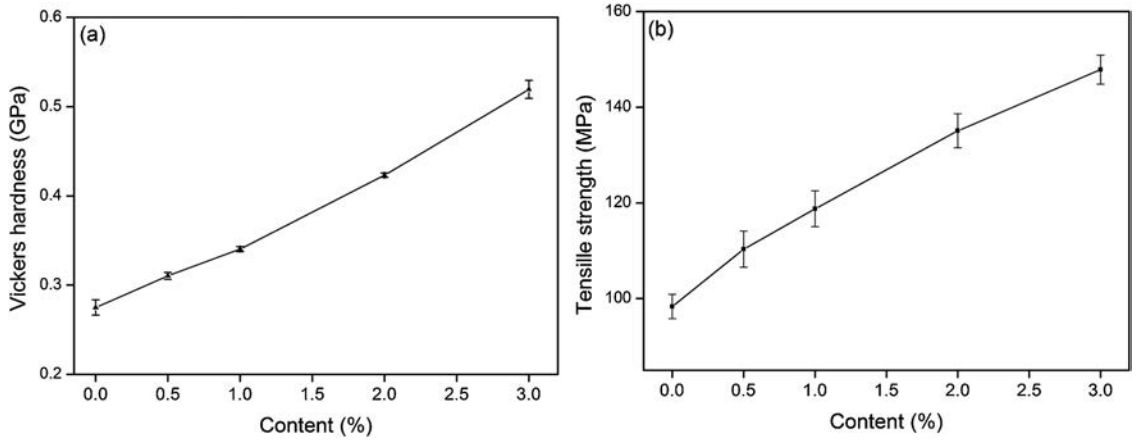

Fig. 2. Mechanical properties of $Ti_3C_2T_x$/Al composites. Vickers hardness (a) and tensile strength (b) as a function of $Ti_3C_2T_x$ content.

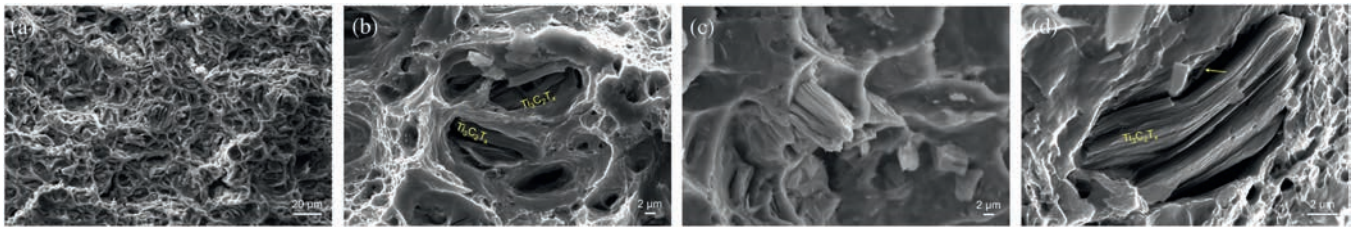

Fig. 3. Fracture surfaces of 3 wt% $Ti_3C_2T_x$/Al composite after tensile test. (a) A low magnification SEM micrograph; (b–d) High magnification SEM micrographs taken from (a).

particles due to the strong interface between $Ti_3C_2T_x$ and Al. As the maximum stress reached, the fracture of reinforcement occurred. However, the fractured $Ti_3C_2T_x$ particles demonstrated a combination feature of delamination, kink layers, and stair fracture surface, which consumes much strain energy during deformation. The above fracture modes endow the composites with improved mechanical properties.

Strength increments of the selected Al matrix composites reinforced with CNTs, graphene (Gr) and $Ti_3C_2T_x$ were compared in Fig. 4 [8,31–38]. 0.5 wt% graphene and less than 2 wt% CNTs are always incorporated in Al matrix to improve the tensile strength because more CNTs and Gr additions cause a decrease in strength of composites due to their agglomeration. Compared with CNT/Al and Gr/Al previously studied composites, $Ti_3C_2T_x$/Al composites

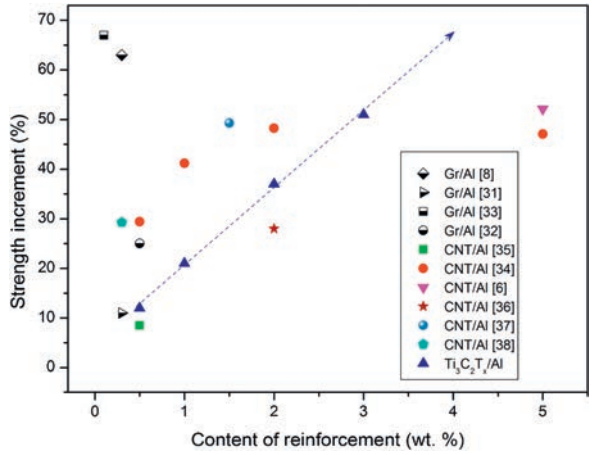

Fig. 4. Comparison of strength increment for Al matrix composites reinforced with CNTs (CNTs/Al), graphene (Gr/Al) and $Ti_3C_2T_x$ ($Ti_3C_2T_x$/Al).

demonstrate a linear increase in the tensile strength with increasing content. In addition, the tensile strength of $Ti_3C_2T_x$/Al composites exhibits a tendency to be further improved with increasing the content of $Ti_3C_2T_x$. Therefore, an obvious advantage of the $Ti_3C_2T_x$/Al composites is that their properties are tunable.

Fig. 5a shows frictional curves of the prepared materials under a load of 5 N. For the pure Al material, the friction coefficient fluctuates greatly during the running period of 300 s. In addition, there is high noise for pure Al during the sliding process. Due to the severe wear, the friction coefficient of pure Al reaches about 0.49. However, for $Ti_3C_2T_x$/Al, the friction coefficient shows a moderately fluctuation, and is about 0.2. This result has been supported by the hardness of 0.52 GPa for the composite, which is higher than 0.27 GPa for pure Al. The 3 wt% $Ti_3C_2T_x$/Al composite undergoes less plastic deformation and exhibits lower friction coefficient as compared with pure Al.

The worn surfaces of prepared materials after dry sliding test have been depicted in Figs. 5b and c. The worn surface of pure Al is severe, and characterized with many shallow grooves along the sliding direction and the welding of removed debris (Fig. 5b). These features indicate that the abrasive wear and the adhesive wear are the main mechanisms for pure Al. Therefore, the friction coefficient of pure Al is high. However, the worn surface of 3 wt% $Ti_3C_2T_x$/Al composite is relatively smooth. The welding of debris on the worn surface are observed (Fig. 5c). The predominant wear mechanism for the $Ti_3C_2T_x$/Al composite is adhesive wear. This mechanism should be ascribed to the solid lubricant effect of $Ti_3C_2T_x$ to reduce friction. During dry sliding test, $Ti_3C_2T_x$ leads to a thin film on the wear surface and reduces the contact area between sliding surfaces. In addition, under the same sliding conditions, the width of wear trace on pure Al material was about 1.86 mm (Fig. 5b), but that on 3 wt% $Ti_3C_2T_x$/Al was about 1.27 mm under the same load of 5 N (Fig. 5c). This feature is due to the higher hardness of composite. The $Ti_3C_2T_x$ reinforcement supports the counterfaces

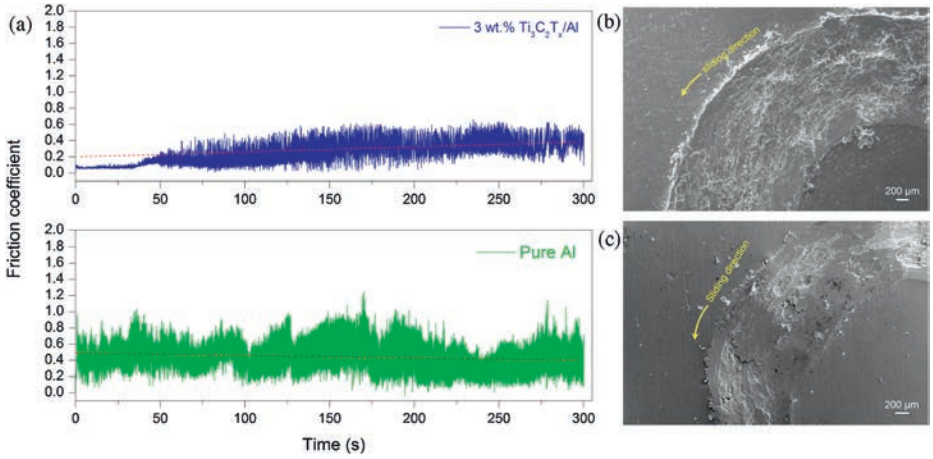

Fig. 5. Frictional curves of pure Al and 3 wt% $Ti_3C_2T_x$/Al composite (a). The average value was estimated with the linear fit (dashed red line). SEM micrographs of the worn surface of pure Al (b) and 3 wt% $Ti_3C_2T_x$/Al composite (c).

and decreases the wear damage. The similar behavior was also found in $Ti_3C_2T_x$/Cu composites [39,40].

In addition, the lubricant effect of MXenes ($Ti_3C_2T_x$ and Ti_2CT_x) has also been confirmed in oil [41–44] and polymer matrix composites [26,27]. $Ti_3C_2T_x$ significantly reduces the friction coefficient of base oil due to the tribofilm formation, which is comparable with graphene. Ti_2CT_x also acts as a self-lubricating additive to enhance the tribological resistance of composites. Ti_3C_2/polyethylene composites have a better friction-reducing performance compared with pure polyethylene due to the formation of Ti_3C_2 lubricating film [26]. Ti_2CT_x/epoxy resin nanocomposites exhibit a great improvement in anti-friction properties [27].

The above results demonstrated that the 2D $Ti_3C_2T_x$ nanosheets, similar to graphene, hexagonal BN, and MoS_2 particles [45], play an effective role in the reinforcement of frictional resistance of Al matrix composites.

In summary, $Ti_3C_2T_x$/Al composites have been prepared by pressureless sintering of $Ti_3C_2T_x$ and Al powders at 650 °C for 1 h in Ar followed by hot extrusion at 460 °C. The rich surface functional groups of $Ti_3C_2T_x$ enhance the wettability between $Ti_3C_2T_x$ and Al. The homogeneous distribution of $Ti_3C_2T_x$ and the formation of strong bonding interfaces in the composites endows the $Ti_3C_2T_x$/Al composites with improved mechanical properties. The Vickers hardness and the tensile strength continuously increase with increasing $Ti_3C_2T_x$ content from 0.5 wt% to 3 wt%. The 3 wt% $Ti_3C_2T_x$/Al composite has the highest hardness of 0.52 GPa and the highest tensile strength of 148 MPa, increased by 92% and 50%, respectively, as compared with the pure Al material. Under dry sliding test, the 3 wt% $Ti_3C_2T_x$/Al composite exhibits a low friction coefficient of 0.2, twice lower than that of pure Al. The low friction coefficient and the improved hardness of composites both contribute to the enhanced frictional resistance. Our work firstly demonstrates that $Ti_3C_2T_x$ is an effective reinforcement to improve mechanical properties, and also an attractive solid lubricant to enhance the frictional properties of Al matrix composite.

Acknowledgements

This work was supported by the National Natural Science Foundation of China (No. 51772020), Beijing Natural Science Foundation (No. 2182058), Beijing Government Funds for the Constructive Project of Central Universities, and Equipment Development Department of the National Military Commission Foundation of China (No. JZX7Y20190262063601).

Appendix A. Supplementary data

Supplementary material related to this article can be found, in the online version, at doi:https://doi.org/10.1016/j.cclet.2019.09.004.

References

[1] S.R. Bakshi, D. Lahiri, A. Agarwal, Int. Mater. Rev. 55 (2010) 41–64.
[2] S.C. Tjong, Mater. Sci. Eng. R 74 (2013) 281–350.
[3] H. Kwon, M. Leparoux, A. Kawasaki, J. Mater. Sci. Technol. 30 (2014) 736–742.
[4] S.F. Bartolucci, J. Paras, M.A. Rafiee, et al., Mater. Sci. Eng. A 528 (2011) 7933–7937.
[5] H. Kwon, M. Estili, K. Takagi, T. Miyazaki, A. Kawasaki, Carbon 47 (2009) 570–577.
[6] C. He, N. Zhao, C. Shi, et al., Adv. Mater. 19 (2007) 1128–1132.
[7] R. Perez-Bustamante, F. Perez-Bustamante, I. Estrada-Guel, et al., Mater. Charact. 75 (2013) 13–19.
[8] J. Wang, Z. Li, G. Fan, et al., Scr. Mater. 66 (2012) 594–597.
[9] Z.Y. Liu, B.L. Xiao, W.G. Wang, Z.Y. Ma, Carbon 50 (2012) 1843–1852.
[10] D.K. Lim, T. Shibayanagi, A.P. Gerlich, Mater. Sci. Eng. A 507 (2009) 194–199.
[11] A. Maqbool, M.A. Hussaina, F.A. Khalida, et al., Mater. Charact. 86 (2013) 39–48.
[12] M. Park, B.H. Kim, S. Kim, et al., Carbon 49 (2011) 811–818.
[13] H.J. Lee, W.S. Choi, T. Nguyen, Y.B. Lee, H. Lee, Carbon 49 (2011) 5150–5157.
[14] B. Anasori, M.R. Lukatskaya, Y. Gogotsi, Nat. Rev. Mater. 2 (2017) 16098.
[15] M. Naguib, V.N. Mochalin, M.W. Barsoum, Y. Gogotsi, Adv. Mater. 26 (2014) 992–1005.
[16] V.M. Hong Ng, H. Huang, K. Zhou, et al., J. Mater. Chem. A 5 (2017) 3039–3068.
[17] H. Liu, X. Zhang, Y. Zhu, et al., Nano-Micro Lett. 11 (2019) 65.
[18] Y. Zhang, L. Wang, N. Zhang, Z. Zhou, RSC Adv. 8 (2018) 19895–19905.
[19] H. Wang, Y. Wu, X. Yuan, et al., Adv. Mater. 30 (2018) 1704561.
[20] X. Zhang, Z. Zhang, Z. Zhou, J. Energy Chem. 27 (2018) 73–85.
[21] M. Naguib, M. Kurtoglu, V. Presser, et al., Adv. Mater. 23 (2011) 4248–4253.
[22] M. Naguib, T. Saito, S. Lai, et al., RSC Adv. 6 (2016) 72069–72073.
[23] P. Sobolciak, A. Ali, M.K. Hassan, et al., PLoS One 12 (2017) 183705/1-18.
[24] W. Zhi, S. Xiang, R. Bian, et al., Comp. Sci. Technol. 168 (2018) 404–411.
[25] Q. Zhao, Q. Zhu, J. Miao, P. Zhang, B. Xu, Nanoscale 17 (2019) 8442–8448.
[26] H. Zhang, L. Wang, Q. Chen, et al., Mater. Des. 92 (2016) 682–689.
[27] H. Zhang, L. Wang, A. Zhou, et al., RSC Adv. 6 (2016) 87341–87352.
[28] M. Fei, R. Lin, Y. Lu, et al., Ceram. Int. 43 (2017) 17206–17210.
[29] X.Y. Si, F.Y. Chen, Q.H. Deng, S.Y. Du, Q. Huang, J. Inorg. Mater. 33 (2018) 603–608.
[30] J. Zhang, S.B. Li, S.J. Hu, Y. Zhou, Mater. 11 (2018) 1979.
[31] M. Rashad, F. Pan, A. Tang, M. Asif, Pro. Nat. Sci. Mater. 24 (2014) 101–108.
[32] L.Y. Zhao, H.M. Lu, Z.J. Gao, Adv. Eng. Mater. 17 (2015) 976–981.
[33] Y. Wang, C. Zhu, T. Lei, Mater. Sci. Eng. Powder Metall. 23 (2018) 518–525.
[34] A.M.K. Esawi, K. Morsi, A. Sayed, M. Taher, S. Lanka, Comp. Sci. Technol. 70 (2010) 2237–2241.
[35] A.M.K. Esawi, B.M. Ei, Comp. Sci. Technol. 68 (2008) 486–492.
[36] R. Pérez-Bustamante, I. Estrada-Guel, P. Amézaga-Madrid, et al., Mater. Sci. Eng. A 502 (2009) 159–163.
[37] F. Rikhtegar, S.G. Shabestari, H. Saghafian, J. Alloys Compd. 723 (2017) 633–641.
[38] J.G. Park, D.H. Keum, Y.H. Lee, Carbon 95 (2015) 690–698.
[39] Y.J. Mai, Y.G. Li, S.L. Li, et al., J. Alloys Compd. 770 (2019) 1–5.
[40] W. Lian, Y. Mai, C. Liu, et al., Ceram. Int. 44 (2018) 20154–20162.
[41] Y. Liu, X. Zhang, S. Dong, Z. Ye, Y. Wei, J. Mater. Sci. 52 (2017) 2200–2209.
[42] J. Yang, B. Chen, H. Song, H. Tang, C. Li, Cryst. Res. Technol. 49 (2014) 926–932.
[43] X. Zhang, M. Xue, X. Yang, et al., RSC Adv. 5 (2015) 2762–2767.
[44] X. Zhang, Y. Guo, Y. Li, Y. Liu, S. Dong, Chin. Chem. Lett. 30 (2019) 502–504.
[45] S. Zhang, T. Ma, A. Erdemir, Q. Li, Mater. Today 26 (2019) 67–86.